Disease Models & Mechanisms 6, 414-423 (2013) doi:10.1242/dmm.010462

A transgenic zebrafish liver tumor model with inducible *Myc* expression reveals conserved Myc signatures with mammalian liver tumors

Zhen Li[1,*], Weiling Zheng[1,*], Zhengyuan Wang[1], Zhiqiang Zeng[1], Huiqing Zhan[1], Caixia Li[1], Li Zhou[1], Chuan Yan[1], Jan M. Spitsbergen[2] and Zhiyuan Gong[1,‡]

SUMMARY

Myc is a pleiotropic transcription factor that is involved in many cellular activities relevant to carcinogenesis, including hepatocarcinogenesis. The zebrafish has been increasingly used to model human diseases and it is particularly valuable in helping to identify common and conserved molecular mechanisms in vertebrates. Here we generated a liver tumor model in transgenic zebrafish by liver-specific expression of mouse *Myc* using a Tet-On system. Dosage-dependent induction of *Myc* expression specifically in the liver was observed in our *Myc* transgenic zebrafish, *TO(Myc)*, and the elevated *Myc* expression caused liver hyperplasia, which progressed to hepatocellular adenoma and carcinoma with prolonged induction. Next generation sequencing-based transcriptomic analyses indicated that ribosome proteins were overwhelmingly upregulated in the *Myc*-induced liver tumors. Cross-species analyses showed that the zebrafish *Myc* model correlated well with *Myc* transgenic mouse models for liver cancers. The *Myc*-induced zebrafish liver tumors also possessed molecular signatures highly similar to human those of hepatocellular carcinoma. Finally, we found that a small Myc target gene set of 16 genes could be used to identify liver tumors due to Myc upregulation. Thus, our zebrafish model demonstrated the conserved role of *Myc* in promoting hepatocarcinogenesis in all vertebrate species.

INTRODUCTION

Liver cancer, mainly hepatocellular carcinoma (HCC), is one of the leading causes of cancer-related death worldwide (Nordenstedt et al., 2010). It generally has a poor prognosis as it is often diagnosed at an advanced stage when treatment is not effective. Tremendous efforts have been made to decipher the molecular mechanisms of HCC, and gene expression profiling of human HCCs has been used to identify subgroups of patients according to etiological factors, early pre-neoplastic lesions, stages of the disease, rate of recurrence and survival (Hoshida et al., 2009; Lee and Thorgeirsson, 2004; Roessler et al., 2010; Wurmbach et al., 2007). In human HCC, *MYC* is commonly amplified and associated with unfavorable prognosis (Abou-Elella et al., 1996). A higher expression level of MYC is associated with more advanced status of HCC (Gan et al., 1993). However, at which stage and to what extent Myc contributes to human HCC is still unclear. Recently, Myc has been suggested to be at the center of human liver tumor malignant conversion, on the basis of genome-wide gene expression profiling (Kaposi-Novak et al., 2009), but this conclusion still lacks experimental confirmation and thus an *in vivo* animal model is highly desired.

In the past decade, the zebrafish has become an increasingly popular experimental model for human diseases (Lieschke and Currie, 2007; Liu and Leach, 2011; Payne and Look, 2009). We have demonstrated that the zebrafish and human liver tumors have molecular conservation at various levels, indicating the potential of zebrafish for modeling human liver cancer (Lam et al., 2006). Although several Myc transgenic mouse models for liver cancers have been reported (Lee et al., 2004), we envision that comparative studies of Myc tumors in an evolutionary distant model such as zebrafish should disclose highly conserved features and biomarkers of Myc tumors. Thus, in the present study, we have generated an inducible *Myc* transgenic zebrafish line and demonstrated that overexpression of Myc in the liver results in obvious liver tumors. Furthermore, by transcriptomic analyses, we found that the zebrafish *Myc* tumor model not only captured the human liver cancer signature but also showed high similarity with mouse *Myc*-induced liver tumor models. We also identified a short list of Myc targets that could be used to predict Myc-causing malignancies. Our analyses suggested that this transgenic zebrafish line could serve as a model for human liver tumors induced by over-activation of *MYC*.

RESULTS

Generation of Tet-On inducible *Myc* transgenic zebrafish, *TO(Myc)*

In order to investigate the role of *Myc* in liver tumorigenesis, a transgenic line, named *TO(Myc)*, was generated by introducing mouse *Myc* cDNA in a Tet-On vector under a liver-specific zebrafish *fabp10* promoter (Her et al., 2003). By whole mount *in situ* hybridization, we confirmed that transgenic *Myc* expression was specifically induced in the liver after doxycycline (Dox) treatment (Fig. 1A,B). To investigate the effect of *Myc* overexpression on liver growth, *TO(Myc)* fish were crossed with

[1]Department of Biological Sciences, National University of Singapore, Singapore
[2]Department of Microbiology and Marine and Freshwater Biomedical Sciences Center, Oregon State University, Corvallis, OR 97331, USA
*These authors contributed equally to this work
‡Author for correspondence (dbsgzy@nus.edu.sg)

Received 26 June 2012; Accepted 16 September 2012

TRANSLATIONAL IMPACT

Clinical issue

Liver cancer is a prominent malignancy, causing more than half a million deaths worldwide every year. Human liver tumors are morphologically and genetically heterogeneous, and the molecular pathogenesis of the disease is highly complex. Transgenic animals with altered expression of key oncogenes provide a tractable system to facilitate the understanding of the complex mechanisms of carcinogenesis. In addition, comparing liver tumors from evolutionarily distinct species, such as fish and human, should help identify more robust and reliable molecular pathways, as well as diagnostic and prognostic biomarkers, for liver cancer.

Results

The authors established an inducible liver cancer model by generating a transgenic zebrafish line in which the mouse *Myc* oncogene was inducibly expressed in the liver by tetracycline treatment [*TO(Myc)* zebrafish]. They observed a dosage-dependent induction of Myc expression with increasing concentrations of doxycycline (a tetracycline derivative), and high levels of Myc expression eventually caused liver tumors in 100% of transgenic zebrafish. Tumors progressed from hepatocellular adenoma to carcinoma with prolonged Myc induction. Cross-species analyses showed that the zebrafish *TO(Myc)* model correlated well with *Myc* transgenic mouse models of liver cancers at the transcriptome level. In addition, the authors found that *Myc*-induced zebrafish liver tumors have molecular signatures that are highly similar to that of human hepatocellular carcinoma. Finally, the authors found that a small subset of 16 Myc target genes could distinguish advanced human hepatocellular carcinoma from low-grade liver tumors.

Implications and future directions

These studies involving a *TO(Myc)* transgenic zebrafish model demonstrate the conserved role of Myc in promoting hepatocarcinogenesis in multiple vertebrate species. The identification of a small subset of Myc target genes might help to establish better prognostic markers for Myc-induced liver tumours.

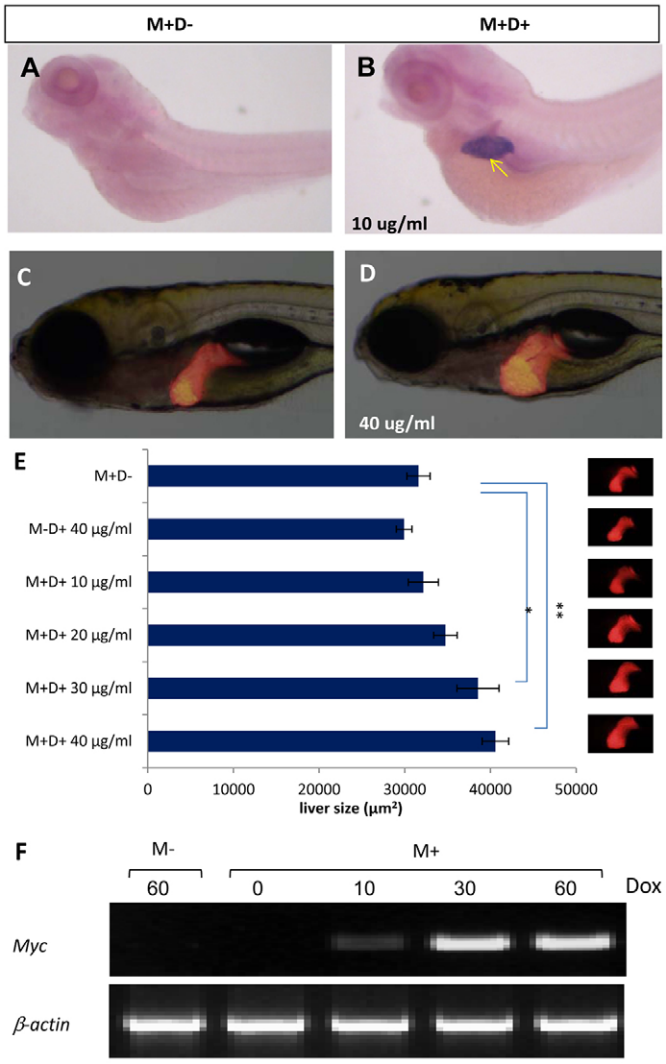

Fig. 1. Inducible *Myc* expression and liver overgrowth in *TO(Myc)* fry. (A,B) Liver-specific *Myc* expression in *TO(Myc)* fry. *Myc* transgenic fry were treated with 10 μg/ml Dox from 2 dpf for two days and liver-specific *Myc* expression was confirmed by whole mount *in situ* hybridization at 4 dpf, as indicated by a yellow arrow. An untreated control is shown in A. (C,D) *In vivo* detection of liver overgrowth in *TO(Myc)* fry. Double transgenic fry from a cross of *TO(Myc)* and LiPan zebrafish were treated with 40 μg/ml Dox and livers were observed by RFP expression (D). An untreated control is shown in C. (E) Dose-dependent growth of liver in *TO(Myc)* fry. *TO(Myc)*/LiPan double transgenic fry were treated with increasing concentrations of Dox; liver imaging is shown in the pictures on the right. 2D measurement of liver areas were performed using ImageJ as described previously (Huang et al., 2012) and the quantitative data are shown on the left. The groups significantly different from the control group (M+D-) by Student's *t*-test are indicated: **P*<0.05; ***P*<0.01. (F) Dose-dependent induction of *Myc* mRNAs in adult livers as detected by RT-PCR. Concentrations of Dox are indicated at top of each lane. M+, *TO(Myc)* fish; M-, non-transgenic siblings; D+, presence of doxycycline; D-, absence of doxycycline. *B-actin* transcripts served as loading controls for RT-PCR.

the LiPan line, which has red fluorescent protein (RFP) expression in the liver to facilitate observation of liver development (Korzh et al., 2008). As shown in Fig. 1D, overgrowth of the liver was apparent after 4 days of Dox (40 μg/ml) treatment starting from 3 dpf (days postfertilization), in comparison with that of untreated controls (Fig. 1C). By using different concentrations of Dox, we observed a clear dose-dependent increase of the liver size in *TO(Myc)* embryos, as indicated by two-dimensional (2D) measurement (Fig. 1E). By contrast, no obvious change was noted in the non-*TO(Myc)* siblings (M-D+) even under high dosage (40 μg/ml) of Dox treatment. Consistent with the observations, the dose-dependent induction of *Myc* transgene expression was also confirmed by reverse transcription polymerase chain reaction (RT-PCR), in which the transgenic embryos were treated with increasing concentrations of Dox (10, 30 and 60 μg/ml) for 2 days from 2 dpf (Fig. 1F). Although there was a dosage-dependent increase of proliferation in the *TO(Myc)* livers after Dox induction, there was no detectable apoptosis in the *TO(Myc)* livers at all concentrations of Dox from 10-60 μg/ml (data not shown).

Induction of liver tumors in *TO(Myc)*

To examine the tumorigenic potency of the *TO(Myc)* line, *TO(Myc)* transgenic zebrafish and their non-transgenic siblings were treated with Dox (60 μg/ml) from 21 dpf. All Dox-treated transgenic fish (M+D+) showed enlarged abdomens (Fig. 2D) and obvious liver overgrowth (Fig. 2E) after only 2-3 weeks of Dox induction (100%, *n*=50) compared to Dox-treated non-transgenic siblings (M-D+) (Fig. 2A,B). Histological analysis of the M+D+ fish showed hyperplasia (HP; 6/10), mixed hyperplasia/hepatocellular adenoma (HP/HCA; 1/10) and adenoma (3/10) (Fig. 2F; Table 1). In general, the entire liver was uniformly

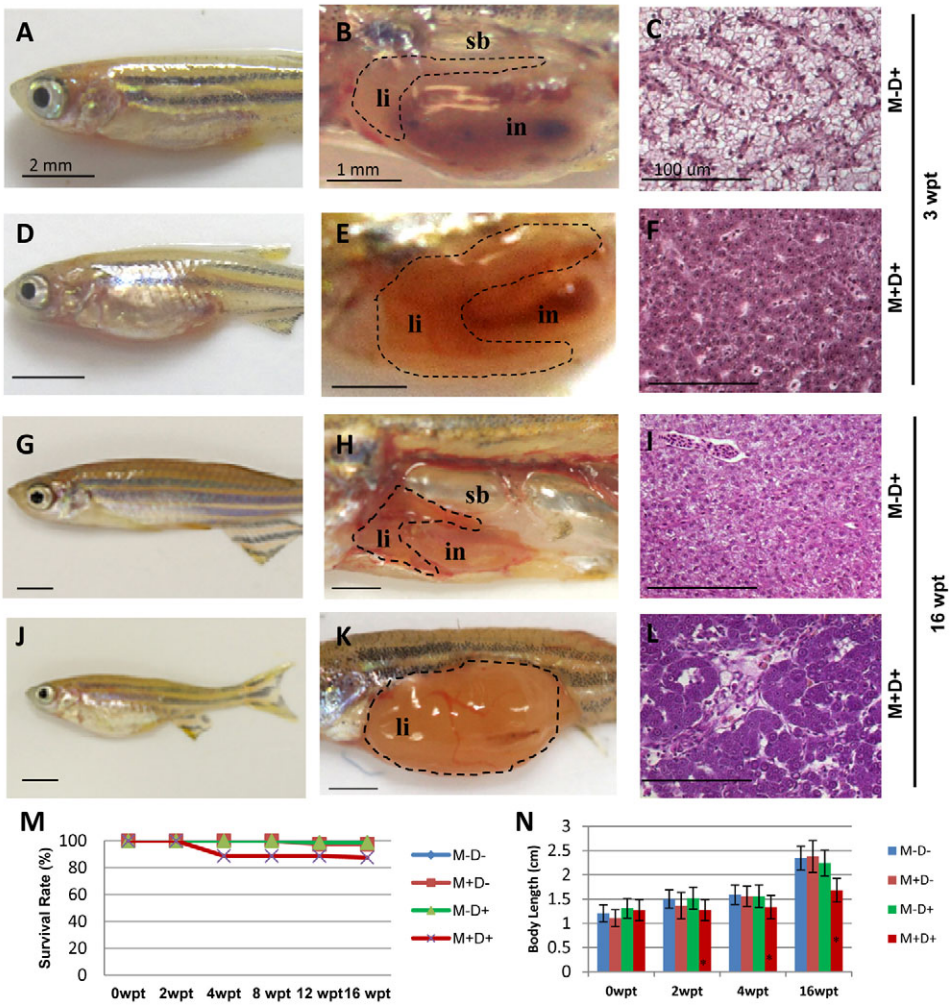

Fig. 2. Induction of liver tumors in *TO(Myc)* fish. (A-L) Transgenic and non-transgenic fish were treated with Dox (60 µg/ml) starting from 21 dpf and sampled at different times. Samples were collected at 3 wpt (A-F) and 16 wpt (G-L). The left column displays external appearance, the middle column shows internal abdominal organs with the livers outlined, and the right column depicts H&E staining of liver sections. At 3 wpt, non-transgenic siblings had normal body shape (A), whereas transgenic fish showed an enlarged belly (D). Dissection of a transgenic fish (E) showed an enlarged abdomen compared to a non-transgenic sibling (B). At 16 wpt, more obviously enlarged abdomen (J) and fully grown liver tumor (K) were observed, in comparison with the controls (G,H). Histological examination confirmed that most transgenic fish developed hyperplasia (F) at 3 wpt and adenoma (L) at 16 wpt in comparison with normal liver histology in non-transgenic siblings (C,I). (M,N) Survival curves (M) and body lengths (N) for the four experimental groups until 16 wpt. Noted body length was significantly different from the control group after just 2 weeks of treatment; **P*<0.0001. li, liver; in, intestine; sb, swimbladder. Scale bars: 2 mm, 1 mm and 100 µm for the left, middle and right columns, respectively.

transformed into tumor phenotype without the existence of normal liver tissue. For observation of the effect of prolonged activation of *Myc*, we treated the fish continuously for up to 16 weeks. The treated fish (M+D+) did not show significant increase in mortality (Fig. 2M), but they did show more prominent liver enlargement (Fig. 2J,K) and significantly smaller body size (Fig. 2J,N) than control fish. Hematoxylin and eosin (H&E) examination of samples from 8 and 16 weeks post-treatment (wpt) revealed a progression of liver tumors from predominantly hyperplasia to adenoma (Table 1). We also noticed one case of early HCC, as shown in Fig. 2L, confirming the liver tumor progression with prolonged *Myc* activation.

Table 1. Progression of Myc-induced liver tumor

Period (wpt)	Group	Histopathological diagnosis (*n*)				
		Normal	HP	HP/HCA	HCA	Early HCC
3	M+D+ (*n*=10)	0	6	1	3	0
	Control (*n*=10)	10	0	0	0	0
8	M+D+ (*n*=8)	0	2	4	2	0
	Control (*n*=10)	10	0	0	0	0
16	M+D+ (*n*=8)	0	0	0	7	1
	Control (*n*=10)	10	0	0	0	0

Controls were untreated non-transgenic siblings (M-D+).

RNA sequencing of *Myc*-induced liver tumors indicated a distinct transcriptomic pattern from control livers

In order to investigate the molecular mechanism of *Myc*-induced liver tumors, livers from all four groups (transgenic and non-transgenic fish, treated or untreated with Dox) were collected after 4 months of Dox-treatment at 60 µg/ml. Two biological replicates (each with four or five pooled livers) were included for each group. About 40 million tags were sequenced for each sample mapped to the zebrafish RefSeq database for quantitative analysis of transcript expression (supplementary material Table S1). To verify the dynamic range of gene expression, reverse-transcription quantitative PCR (RT-qPCR) was performed for several selected genes with a range of 249,696 to 0.12 TPM (transcripts per million) in the control sample 1 (M-D-_1). As shown in Fig. 3A, there was a good correlation of the RNA sequencing data and RT-qPCR results.

To compare the molecular similarity of the tumor and control samples, whole transcriptomic data from all eight samples were subjected to hierarchical clustering using MeV software (Saeed et al., 2006; Saeed et al., 2003). As shown in Fig. 3B, the two tumor samples (M+D+) were clustered as an independent branch and were

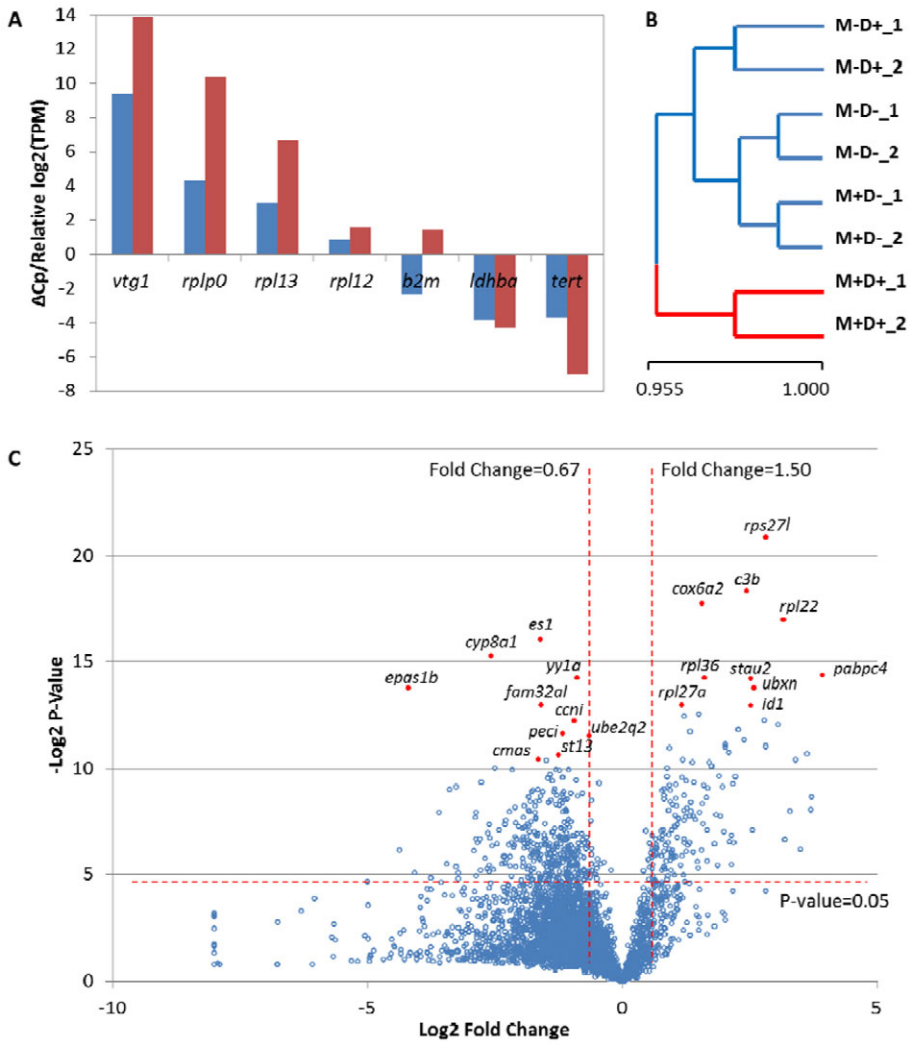

Fig. 3. Validation and characterization of RNA sequence tags. (A) qPCR validation of RNA-SAGE results using untreated wild-type samples. The blue bars represent normalized ΔCp values from the qPCR results, and the red bars are logarithm-transformed (base 2) TPM values. Both ΔCp and TPM values are normalized against the ΔCp and TPM of bactin. (B) Hierarchial clustering of the eight samples. (C) Volcano plot showing the distribution of transcripts over different fold changes and *P*-values between control and tumor samples. The top ten up- and downregulated transcripts, ranked by their distance to the base point, are marked in red.

well separated from all control samples (M-D-, M-D+ and M+D-), suggesting that there were substantial changes in the tumor transcriptome.

Differentially expressed genes in *Myc*-induced liver cancer

In order to identify the genes important for liver cell transformation, a *t*-test was performed between the six control and two tumor samples. Differentially expressed genes were selected by accepting a *P*-value of <0.05 and fold change >1.5 for further analyses. In order to focus on physiologically relevant genes, we also set an expression level cutoff at an average of 10 TPM in either control or tumor samples, which is equivalent to about three transcripts per cell, based on an estimation of 300,000 transcripts per cell (Mortazavi et al., 2008). Finally, 148 up- and 353 downregulated transcript entries were selected using these criteria (supplementary material Tables S2, S3). These up- and downregulated zebrafish genes were subsequently mapped to 125 and 207 human gene symbols. As illustrated in the volcano plot (Fig. 3C), there were fewer upregulated genes than downregulated genes, but the upregulated genes were more deregulated as judged by their distances from the base point.

To understand the composition of these differentially expressed genes, Gene Ontology Slim classification analysis was performed (Fig. 4A-C). Interestingly, all genes in the macromolecular complex and ribosome groups were upregulated (Fig. 4B). By contrast, more genes involved in nucleotide binding, ion binding, protein binding, transferase activity, hydrolase activity, transporter activity, membrane and nucleus were downregulated. It is also interesting to note that there were more uncharacterized genes in the downregulated group than the upregulated group, probably implying that less attention was devoted to the downregulated genes in the *Myc* pathway and cancers in previous studies.

To gain more detailed functional insights into the differentially expressed gene list, gene ontology enrichment analysis was conducted. As shown in Table 2, ribosome and translation are the most prominent groups in the upregulation division. Consistent with this, all of the 59 ribosomal protein genes identified showed upregulation in the tumors (Fig. 4D). Of these, 34 genes (*rpl4*/*5a*/*7a*/*8*/*9*/*10a*/*11*/*12*/*13*/*13a*/*18a*/*19*/*21*/*22*/*26*/*27a*/*34*/*36*/*36a* and rps*3*/*5*/*7*/*8*/*11*/*12*/*13*/*14*/*15*/*16*/*20*/*21*/*23*/*25*/*29*) and several major translation factors (*eif2s1*/*3*, *eif3c*/*d*/*ea*/*ha*, *eef1g* and *ef1a*) were present in the significantly upregulated group in the tumors (supplementary material Table S2).

We also compared the expression of endogenous myc genes. Out of the six members of the myc gene family in zebrafish (*myca, mycb,*

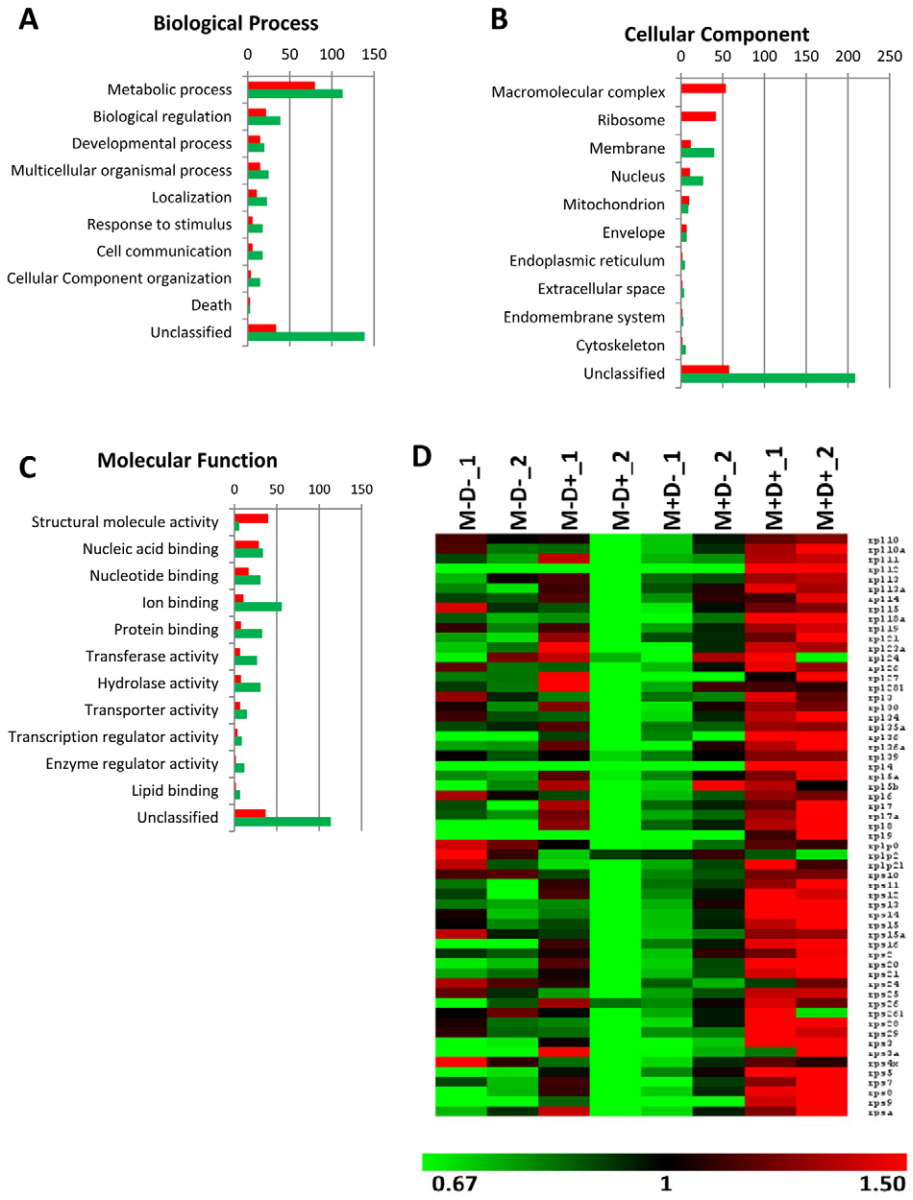

Fig. 4. Functional classification and visualization of differentially expressed genes. (A-C) Gene Ontology Slim classification of the up- and downregulated genes in *Myc*-induced liver tumors. Red and green bars represent up- and downregulated genes, respectively, in the three categories: biological process (A), cellular component (B) and molecular function (C). Numbers of genes are indicated at the top. (D) Heat map of ribosomal protein mRNA expression profiles. The eight individual samples are indicated at the top of each column and the gene names of ribosomal proteins are given on the right. Red and green represent up- and downregulation as indicated in the bar below. The numbers were calculated by dividing the TPM in one sample by the average TPM of the same transcripts across all eight samples.

mych, mycl1a, mycl1b and *mycn*), only *mycb* and *mych* were relatively highly expressed in the liver, with averages of 54.9 and 13.3 TPM, respectively, in the control samples (M-D-, M-D+ and M+D-) although these decreased to 13.3 and 3.5 TPM, respectively, in the liver tumor samples (M+D+). Thus, it seems that high level of transgenic expression of the mouse Myc negatively affects the expression of endogenous myc genes. By contrast, all the rest of the myc genes had extremely low expression level (0.0 to 2.3 TPM) in all the liver samples (control and tumor). Thus, it is impossible to evaluate their change during tumorigenesis.

Myc zebrafish model shows good correlation with *Myc*-induced mouse transgenic model

We next examined the similarity of *Myc* zebrafish model to various mouse HCC models, including two chemically induced [ciprofibrate (CIP) and diethylnitrosamine (DENA)], four transgenic (overexpression of *Myc*, *E2f1*, *Myc*/*E2f* or *Myc*/*Tgfa* in the liver) and one knockout (*Acox1*$^{-/-}$) models (Lee et al., 2004). Hierarchical clustering analysis of gene expression patterns was used to assess the relative similarities between different mouse HCC models. Three distinctive HCC clusters were identified. Our *Myc* overexpression-induced liver cancer clearly distinguished the *Myc-E2f1-Myc*/*E2f1* cluster from the other models, and it showed the highest relatedness to *Myc*/*E2f1* transgenic mice, suggesting conservation of *Myc* signatures between zebrafish and mice liver tumors induced by overexpression of *Myc* (Fig. 5A; supplementary material Table S4). Thus, our zebrafish model successfully resembles mouse liver tumor under similar a inducer (here *Myc*) and confirmed conservation between zebrafish and mouse liver cancers.

Myc-induced zebrafish liver tumors show the highest transcriptome similarity to HCC

Hepatocarcinogenesis is a multistage process following a dysplasia-adenoma-carcinoma sequence with distinct morphological and

Table 2. Gene Ontology enrichment analysis of differentially expressed genes in *Myc*-induced zebrafish liver tumors

	Term	Count	%	*P*-value
Up				
Biological process	GO:0006412~translation	49	33.8	1.01E-44
	GO:0006413~translational initiation	6	4.1	5.48E-05
	GO:0051726~regulation of cell cycle	6	4.1	3.95E-04
Molecular function	GO:0005840~ribosome	40	27.6	8.95E-38
	GO:0030529~ribonucleoprotein complex	41	28.3	4.41E-31
	GO:0043228~non-membrane-bounded organelle	44	30.3	2.86E-18
	GO:0043232~intracellular non-membrane-bounded organelle	44	30.3	2.86E-18
	GO:0033279~ribosomal subunit	9	6.2	4.32E-09
	GO:0015935~small ribosomal subunit	7	4.8	2.46E-08
	GO:0005852~eukaryotic translation initiation factor 3 complex	6	4.1	7.45E-07
	GO:0005746~mitochondrial respiratory chain	3	2.1	5.28E-03
Cellular component	GO:0005840~ribosome	40	27.6	8.95E-38
	GO:0030529~ribonucleoprotein complex	41	28.3	4.41E-31
	GO:0043228~non-membrane-bounded organelle	44	30.3	2.86E-18
	GO:0043232~intracellular non-membrane-bounded organelle	44	30.3	2.86E-18
	GO:0033279~ribosomal subunit	9	6.2	4.32E-09
	GO:0015935~small ribosomal subunit	7	4.8	2.46E-08
	GO:0005852~eukaryotic translation initiation factor 3 complex	6	4.1	7.45E-07
	GO:0005746~mitochondrial respiratory chain	3	2.1	5.28E-03
Down				
Biological process	GO:0055114~oxidation reduction	36	10.32	2.30E-12
	GO:0006631~fatty acid metabolic process	5	1.43	9.59E-03
Molecular function	GO:0009055~electron carrier activity	17	4.87	2.42E-06
	GO:0005506~iron ion binding	19	5.44	9.23E-06
	GO:0020037~heme binding	13	3.72	1.12E-05
	GO:0046906~tetrapyrrole binding	13	3.72	1.85E-05
	GO:0004866~endopeptidase inhibitor activity	9	2.58	2.16E-04
	GO:0004857~enzyme inhibitor activity	10	2.87	4.32E-04
	GO:0030414~peptidase inhibitor activity	9	2.58	4.73E-04
	GO:0016712~oxidoreductase activity, acting on paired donors, with incorporation or reduction of molecular oxygen, reduced flavin or flavoprotein as one donor, and incorporation of one atom of oxygen	5	1.43	1.19E-03
	GO:0004867~serine-type endopeptidase inhibitor activity	6	1.72	3.78E-03
	GO:0016860~intramolecular oxidoreductase activity	4	1.15	8.91E-03

molecular signatures. Therefore, we compared the transcriptome of *Myc*-induced zebrafish liver tumors with those from different stages of human liver conditions: low grade dysplastic nodules (LGDN), high grade dysplastic nodules (HGDN), and very early, early, advanced and very advanced hepatocellular carcinoma (veHCC, eHCC, aHCC and vaHCC) (Table 3). In the first human HCC dataset (GSE12443) (Kaposi-Novak et al., 2009), the upregulated genes of *Myc*-induced zebrafish tumors clearly distinguished HGDN and eHCCs from others, and they showed significant similarity to eHCC. Another human HCC dataset (GSE6764) included more advanced HCC stages, in which the pathological HCC stages were defined by tumor size, differentiation status and metastasis level (Wurmbach et al., 2007). Similarly, the upregulated genes of the zebrafish tumors successfully captured human HCC but not the less severe groups including HCA (Fig. 5B; Table 3). Within the HCC group, it showed the highest similarity with very advanced human HCC. Analyses of the leading edge genes revealed that most of them are involved in mRNA transcription (*SND1, BTF3, MED30, EXOSC3*), rRNA processing (*EXOSC3, NAS2*), protein translation and folding (*RPSs, RPLs, EIF3, EEF1, CCT2, CCT6A, CCT8*), cell cycle regulation (*CAPRIN1, GNB2L1, CGREF1, DTYMK, PCNP*) and mitochondrial function (*SND1, CHCHD3, PDSS, SLC25A39*) (supplementary material Table S5).

A 16-gene signature can be used to classify advanced stages of HCC

Myc is a global transcription factor, therefore it is interesting to examine the Myc target genes involved in hepatocarcinogenesis. Thus, the upregulated genes from the *Myc*-induced zebrafish liver

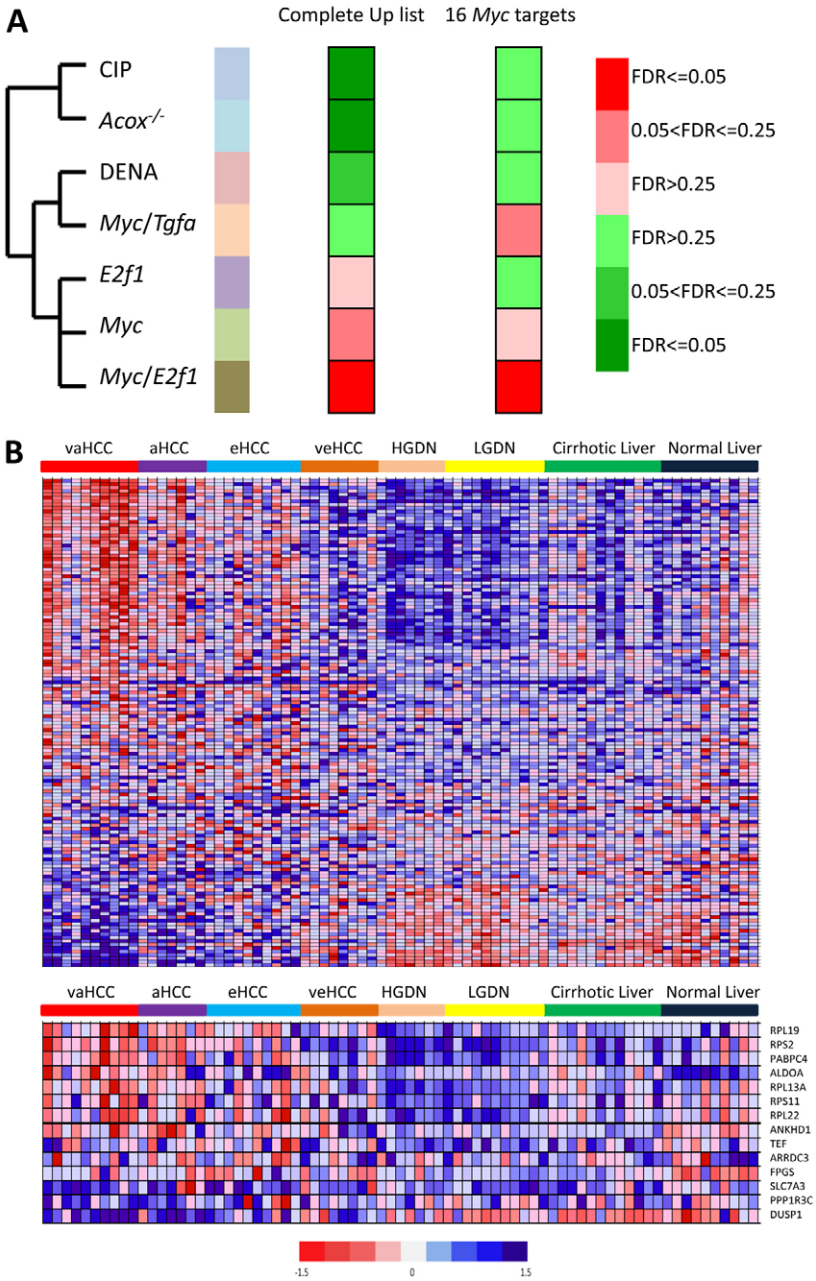

Fig. 5. Comparison of *Myc*-induced zebrafish liver tumors with different stages of human HCC and seven mouse HCC models. (A) Comparison of *Myc*-induced zebrafish liver cancer with seven mouse models. Hierarchical clustering of the seven mouse models were adapted from a previous publication (Lee et al., 2004). The level of similarity of *Myc*-induced zebrafish liver cancer and different mouse models are shown in different colors, with red indicating positive correlation and green indicating negative correlation. (B) Heat map showing expression patterns of 125 Myc upregulated genes (top) and 16 target genes (bottom) in different human conditions. The scale bar represents up- (red) or down- (blue) regulation of genes with fold change in log2 ratio.

tumors were compared with Myc target genes retrieved from the Molecular Signatures Database (MSigDB) (Subramanian et al., 2005), where 382 Myc targeted genes could be mapped by the zebrafish transcripts in the RefSeq database. We found that 16 of them presented in the 125 upregulated genes from the Myc-induced zebrafish tumors, including genes encoding ribosomal proteins (*RPL13A*, *RPL19*, *RPL22*, *RPS2*, *RPS11*, *RPS28*), mitochondria (*FPGS, SLC7A3, ALDOA*), translation (*PABPC4, ANKHD1*), cell cycle inhibition (*DUSP1, CGREF1*), glycogen biosynthesis (*PPP1R3C*), transcription factor (*TEF*) and a member of the arrestin family (*ARRDC3*). Notably, *DUSP1* and *ARRDC3* have been suggested as tumor suppressors (Calvisi et al., 2008; Draheim et al., 2010). We also performed gene set enrichment analysis (GSEA) using these 16 genes as *Myc* signature to classify different mouse HCC models and various stages of human HCCs (Fig. 5B; Table 3). The 16-gene signature showed a better prediction of Myc transgenic mice (Fig. 5A). Interestingly, these 16 genes also clearly distinguish HCC with less severe human liver tumors, with better correlation to more advanced HCC (Fig. 5B; Table 2). Therefore, the 16-gene signature could potentially be used as a molecular prognosis signature for human HCC patients.

Similarly, we also compared the 125 upregulated genes from our data with another set of Myc target genes (Zeller et al., 2003) (http://www.myc-cancer-gene.org/index.asp), whereby 681 genes were identified with zebrafish homologs and 24 of them were overlapped (indicated by asterisks in supplementary material Table S2), including five genes (*RPL13A*, *RPL19*, *RPL22*, *RPS11* and *FPGS*) in the earlier-identified 16-gene list. We found that the 24 genes

Table 3. Comparison of *Myc*-induced zebrafish liver tumors with different stages of human hepatocarcinogenesis using gene set enrichment analysis

		Complete up list[a]		16 Myc targets[b]	
Dataset	**Tumor status**	**NES**	**FDR**	**NES**	**FDR**
GSE12443	CN	–2.45	<0.001	–1.56	0.055
	LGDN	–1.62	<0.001	0.46	0.984
	HGDN	1.19	0.063	–0.29	0.717
	Early HCC	2.17	<0.001	1.37	0.133
GSE6764	CN	–1.40	0.005	–1.11	0.352
	LGDN	–1.42	0.001	–1.65	0.004
	HGDN	–1.34	0.004	–1.83	0.001
	Very early HCC	–1.74	<0.001	–1.26	0.186
	Early HCC	1.09	0.236	0.93	0.527
	Advanced HCC	1.48	0.009	1.36	0.109
	Very advanced HCC	1.65	<0.001	1.52	0.047
GSE11819	HCA	0.59	1.000	–0.75	0.798
GSE7473 GPL96	HCA	0.95	0.570	–0.88	0.598
GSE7473 GPL3283	HCA	–1.33	0.062	–0.75	0.829

[a]Analysis was carried out using the complete list of 125 genes upregulated in *Myc*-induced zebrafish tumors.
[b]Analysis was carried out using the 16 common Myc target genes based on this study and the Molecular Signatures Database.
CN, cirrhotic nodules.

also showed a better prediction of Myc transgenic mice (supplementary material Table S4) and high correlation with advanced and very advance HCC (supplementary material Table S5) as compared with the entire upregulated gene list.

DISCUSSION

By generating a transgenic zebrafish model and utilizing RNA-sequencing technology, we have examined the transcriptome of zebrafish liver tumors driven by the oncogene *Myc*. Our analyses have shown that ribosome biogenesis constitutes the key features of *Myc*-mediated liver tumors. Cross-species analyses showed that the zebrafish *Myc* model correlated well with *Myc* transgenic mouse models for liver cancer. We also illustrated that the *Myc*-induced zebrafish liver tumors possessed molecular signatures common to human HCC. Interestingly, a small set of 16 Myc target genes was identified that could be further tested as HCC prognosis markers in clinical samples.

Consistent with previous reports that MYC is the key regulator of ribosome gene expression and protein translation (van Riggelen et al., 2010), we observed that essentially all ribosomal protein genes as well as several translation factor genes were upregulated. The ribosome is the machinery for protein synthesis; therefore, upregulation of ribosome gene expression could reflect the requirement for increased cell proliferation. This is in contrast to our two other liver tumor models induced by overexpression of $kras^{v12}$ or *xmrk* in transgenic zebrafish (Li et al., 2012; Nguyen et al., 2011; Nguyen et al., 2012), which also showed prominent cell proliferation and liver overgrowth but did not show such obvious upregulation of ribosome genes (data not shown). Thus, the upregulation of ribosome genes in the *Myc* transgenic zebrafish model should be a specific event elicited by the Myc pathway and thus suggests extra-ribosomal functions for these ribosomal proteins. Extra-ribosomal functions have been found in both prokaryotes and eukaryotes and include regulation of their own transcription and translation, DNA repair endonuclease activity and modulation of gene-specific transcription and translation, such as sequestering MDM, protecting p53 and sequestering their activator Myc (Lindström, 2009; Ruggero and Pandolfi, 2003). Consistent with these reports, we observed obvious upregulation of *rpl11*, which can bind to Myc and inhibit its function. In addition, *rpl26* and *rps7*, whose homologs have been shown to inhibit MDM2 and to protect p53, were also upregulated. Moreover, among the significantly upregulated ribosome genes, *rpl12*, *rpl13*, *rpl36a* and *rps8* have also been reported to be upregulated in human HCC (Kondoh et al., 2001).

Although liver tumorigenesis progressed with time in the *TO(Myc)* line, we observed mostly hepatocellular adenoma after 4 months of treatment, despite the fact that the same mouse *Myc* gene expressed in lymphocytes causes leukemia in transgenic zebrafish (Langenau et al., 2005; Langenau et al., 2003). By contrast, transgenic expression of $kras^{v12}$ or *xmrk* alone is sufficient to induce HCC in transgenic zebrafish (Li et al., 2012; Nguyen et al., 2011; Nguyen et al., 2012), suggesting that these oncogenes function distinctively in different tissues and possess different potencies to drive liver tumorigenesis. Similar to our model, Sawey et al. reported that an embryonic hepatoblast cell line lacking *P53* and overexpressing *Myc* was not tumorigenic *in vivo* in the mouse model. By introducing other mutations or transgenes, these cells provide a sensitized background where a single additional oncogenic factor can trigger tumorigenesis (Sawey et al., 2011). In contrast to the histopathological diagnosis, our comparative transcriptomic analyses showed that the *Myc*-induced zebrafish liver tumors captured the molecular signatures of advanced HCCs, suggesting that upregulation of *Myc* signatures are often correlated with malignancy status. In accordance with this speculation, a global gene expression analysis showed that the activation of the *MYC* transcription signature was strongly associated with malignant conversion of liver cancer (Felsher and Bishop, 1999; Jain

et al., 2002; Kaposi-Novak et al., 2009; Shachaf et al., 2004). Thus, our *TO(Myc)* line could serve as a good driving line for hepatocarcinogenesis. Upregulated Myc can affect multiple hallmark capabilities, such as proliferative signaling, energy metabolism, angiogenesis, invasion and survival (Hanahan and Weinberg, 2011). By crossing the *Myc* transgenic line with other transgenic or mutant lines, the progress of hepatocarcinogenesis could be accelerated, as we observed in a $p53^{-/-}$ background (our unpublished data). It could also provide a sensitized background in which a single additional deregulated oncogene can trigger tumorigenesis, thus enabling new oncogenes to be uncovered and studied in the economical and potentially high-throughput zebrafish model. Recently, myc transgenic medaka with liver hyperplasia have also been reported (Menescal et al., 2012) and consistent observations were produced from the two complementing transgenic fish models. It is also interesting to note that Myc-induced mouse HCCs could be rapidly regressed after inactivation of Myc expression (Felsher, 2010; Jain et al., 2002; Shachaf et al., 2004). We also observed a rapid liver tumor regression from our *TO(Myc)* transgenic zebrafish after removal of Dox (data not shown), similar to earlier reported liver tumor regression from our *TO(xmrk)* transgenic zebrafish (Li et al., 2012).

MATERIALS AND METHODS

Generation of Tg(fabp10:TA; TRE:Myc; krt4:GFP) zebrafish

Zebrafish were maintained in compliance with Institutional Animal Care and Use Committee (IACUC) guidelines. Transgenic founders (F0) were generated by co-injection into one-cell stage embryos of three plasmid constructs: pFABP10-rtTA2s-M2 [a 2-kb zebrafish *fabp10* promoter (Her et al., 2003) in prtTA2s-M2 (ClonTech)], pTRE-Myc [full-length mouse *Myc* cDNA in pTRE2 (ClonTech)] and pKRT4-GFP (Gong et al., 2002) (GFP marker for transgenic screening). Injected embryos were raised to adulthood and F0 founders were crossed with wild-type fish for transgenic screening. PCR was conducted on GFP-positive embryos to confirm the co-segregation of these three plasmids. A positive F0 fish was used to establish a stable *Tg(fabp10:TA; TRE:Myc; krt4:GFP)* transgenic line, known as *TO(Myc)*. We always observed a co-segregation of the three plasmids and standard Mendelian inheritance ratios for a single transgenic locus in subsequent generations.

Doxycycline induction and histology analysis

Dox treatment was conducted in six-well plates for embryos and in 6-l tanks for juveniles and adults, with different concentrations of Dox (Sigma-Aldrich). Water was changed every other day. Fish density was ~60 juveniles or ~25 adults per tank. Fish samples were fixed in either Bouin's fixative or formalin solution (Sigma-Aldrich). Sections (5 μm) were processed using the Reichert-Jung 2030 BIOCUT Microtome and stained with Mayer's H&E.

RNA sample preparation and SAGE library sequencing

Liver tumors (M+D+) and three non-tumor control livers (M-D-, M-D+ and M-D+) were prepared for RNA extraction. Four to five livers were pooled for each RNA extraction. Total RNA was extracted using TRIzol Reagent (Invitrogen) and treated with DNase I (Invitrogen) to remove genomic DNA contamination. Total RNA samples were then submitted to Mission Biotech, Taiwan, for SOLiD-based SAGE sequencing. Briefly, mRNA was purified using Dynabeads Oligo(dT) EcoP (Invitrogen) and subjected to cDNA synthesis. Resultant cDNA was digested by *Nla*III and then sequencing adapters were added to the cDNA fragments.

Sequence tag mapping and annotation

The tags were mapped to the zebrafish Reference Sequence database with a criterion of allowing maximum two nucleotide mismatches. Uniquely mapped tag counts for each transcript were normalized to TPM to facilitate comparison between different samples. To eliminate transcripts with only marginal expression, the expression level of the transcripts had to be above 10 TPM in at least one group of samples (control or treated) in order to be included in subsequent bioinformatics analyses. Because sequence tags for vitellogenins were highly variable in different samples, these vitellogenin tags were excluded in all subsequent transcriptomic analyses. To facilitate functional implications of zebrafish transcriptome, all zebrafish genes were mapped to annotated human and mouse genes in order to use existing online software developed for human genes. Thus, Unigene annotation of zebrafish transcript entries were retrieved from the UniGene database and human and mouse homology mapping of zebrafish Unigene clusters were retrieved from the HomoloGene database. For Unigene clusters mapped by more than one transcript entries, the highest TPM value was used to represent the expression level of the Unigene cluster (van Ruissen et al., 2005). Functional characterization of Unigene clusters was based on Gene Ontology classification and can be obtained from Stanford's SOURCE database (Diehn et al., 2003).

Bioinformatic analyses

Gene ontology enrichment analysis was performed using DAVID (Database for Annotation, Visualization and Integrated Discovery) (Huang et al., 2009) with the total zebrafish genome information as the background and *P*-values representing a modified Fisher's exact *t*-test. Gene Ontology Fat categories were used for this analysis. The cutoff for *P*-values was 0.01. We used GSEA to establish the relatedness between zebrafish and mammalian liver cancers (Subramanian et al., 2005). Mammalian liver cancer transcriptome data were retrieved from the Gene Expression Omnibus (GEO) database. These data include different stages of human HCCs (GSE12443, GSE6764), human HCAs (GSE11819, GSE7473) and several mouse HCC models (GSE1897) (Kaposi-Novak et al., 2009; Lee et al., 2004; Rebouissou et al., 2009; Rebouissou et al., 2007; Wurmbach et al., 2007). The statistical significance of the normalized enrichment score (NES) was estimated by using an empirical phenotype-based permutation test procedure. A false discovery rate (FDR) value was provided by introducing adjustment of multiple hypothesis testing.

ACKNOWLEDGEMENTS

The RNA sequencing data reported in this study have been submitted to the Gene Expression Omnibus with access number GSE40745.

COMPETING INTERESTS

The authors declare that they do not have any competing or financial interests.

AUTHOR CONTRIBUTIONS

Z.L. designed experiments, generated liver tumors and RNA sequencing data, and wrote manuscript; W.Z. and Z.W. analyzed RNA sequencing data and wrote the

manuscript; Z.Z. generated transgenic zebrafish; H.Z. optimized tumor induction conditions; C.L. carried out tumor induction experiments and molecular validation; L.Z. and C.Y. carried out characterization of early tumor induction experiments; J.M.S. analyzed tumor histopathology; and Z.G. designed experiments, wrote and finalized the manuscript.

FUNDING

This work was supported by grants from the Biomedical Research Council of Singapore and National Medical Research Council of Singapore [R154000547511].

SUPPLEMENTARY MATERIAL

Supplementary material for this article is available at http://dmm.biologists.org/lookup/suppl/doi:10.1242/dmm.010462/-/DC1

REFERENCES

Abou-Elella, A., Gramlich, T., Fritsch, C. and Gansler, T. (1996). c-myc amplification in hepatocellular carcinoma predicts unfavorable prognosis. *Mod. Pathol.* **9**, 95-98.

Calvisi, D. F., Pinna, F., Meloni, F., Ladu, S., Pellegrino, R., Sini, M., Daino, L., Simile, M. M., De Miglio, M. R., Virdis, P. et al. (2008). Dual-specificity phosphatase 1 ubiquitination in extracellular signal-regulated kinase-mediated control of growth in human hepatocellular carcinoma. *Cancer Res.* **68**, 4192-4200.

Diehn, M., Sherlock, G., Binkley, G., Jin, H., Matese, J. C., Hernandez-Boussard, T., Rees, C. A., Cherry, J. M., Botstein, D., Brown, P. O. et al. (2003). SOURCE: a unified genomic resource of functional annotations, ontologies, and gene expression data. *Nucleic Acids Res.* **31**, 219-223.

Draheim, K. M., Chen, H. B., Tao, Q., Moore, N., Roche, M. and Lyle, S. (2010). ARRDC3 suppresses breast cancer progression by negatively regulating integrin beta4. *Oncogene* **29**, 5032-5047.

Felsher, D. W. (2010). MYC inactivation elicits oncogene addiction through both tumor cell-intrinsic and host-dependent mechanisms. *Genes Cancer* **1**, 597-604.

Felsher, D. W. and Bishop, J. M. (1999). Reversible tumorigenesis by MYC in hematopoietic lineages. *Mol. Cell* **4**, 199-207.

Gan, F. Y., Gesell, M. S., Alousi, M. and Luk, G. D. (1993). Analysis of ODC and c-myc gene expression in hepatocellular carcinoma by in situ hybridization and immunohistochemistry. *J. Histochem. Cytochem.* **41**, 1185-1196.

Gong, Z., Ju, B., Wang, X., He, J., Wan, H., Sudha, P. M. and Yan, T. (2002). Green fluorescent protein expression in germ-line transmitted transgenic zebrafish under a stratified epithelial promoter from keratin8. *Dev. Dyn.* **223**, 204-215.

Hanahan, D. and Weinberg, R. A. (2011). Hallmarks of cancer: the next generation. *Cell* **144**, 646-674.

Her, G. M., Chiang, C. C., Chen, W. Y. and Wu, J. L. (2003). In vivo studies of liver-type fatty acid binding protein (L-FABP) gene expression in liver of transgenic zebrafish (Danio rerio). *FEBS Lett.* **538**, 125-133.

Hoshida, Y., Nijman, S. M., Kobayashi, M., Chan, J. A., Brunet, J. P., Chiang, D. Y., Villanueva, A., Newell, P., Ikeda, K., Hashimoto, M. et al. (2009). Integrative transcriptome analysis reveals common molecular subclasses of human hepatocellular carcinoma. *Cancer Res.* **69**, 7385-7392.

Huang, W., Sherman, B. T. and Lempicki, R. A. (2009). Systematic and integrative analysis of large gene lists using DAVID bioinformatics resources. *Nat. Protoc.* **4**, 44-57.

Huang, X., Zhou, L. and Gong, Z. (2012). Liver tumor models in transgenic zebrafish: an alternative in vivo approach to study hepatocarcinogenes. *Future Oncol.* **8**, 21-28.

Jain, M., Arvanitis, C., Chu, K., Dewey, W., Leonhardt, E., Trinh, M., Sundberg, C. D., Bishop, J. M. and Felsher, D. W. (2002). Sustained loss of a neoplastic phenotype by brief inactivation of MYC. *Science* **297**, 102-104.

Kaposi-Novak, P., Libbrecht, L., Woo, H. G., Lee, Y. H., Sears, N. C., Coulouarn, C., Conner, E. A., Factor, V. M., Roskams, T. and Thorgeirsson, S. S. (2009). Central role of c-Myc during malignant conversion in human hepatocarcinogenesis. *Cancer Res.* **69**, 2775-2782.

Kondoh, N., Shuda, M., Tanaka, K., Wakatsuki, T., Hada, A. and Yamamoto, M. (2001). Enhanced expression of S8, L12, L23a, L27 and L30 ribosomal protein mRNAs in human hepatocellular carcinoma. *Anticancer Res.* **21**, 2429-2433.

Korzh, S., Pan, X., Garcia-Lecea, M., Winata, C. L., Pan, X., Wohland, T., Korzh, V. and Gong, Z. (2008). Requirement of vasculogenesis and blood circulation in late stages of liver growth in zebrafish. *BMC Dev. Biol.* **8**, 84.

Lam, S. H., Wu, Y. L., Vega, V. B., Miller, L. D., Spitsbergen, J., Tong, Y., Zhan, H., Govindarajan, K. R., Lee, S., Mathavan, S. et al. (2006). Conservation of gene expression signatures between zebrafish and human liver tumors and tumor progression. *Nat. Biotechnol.* **24**, 73-75.

Langenau, D. M., Traver, D., Ferrando, A. A., Kutok, J. L., Aster, J. C., Kanki, J. P., Lin, S., Prochownik, E., Trede, N. S., Zon, L. I. et al. (2003). Myc-induced T cell leukemia in transgenic zebrafish. *Science* **299**, 887-890.

Langenau, D. M., Feng, H., Berghmans, S., Kanki, J. P., Kutok, J. L. and Look, A. T. (2005). Cre/lox-regulated transgenic zebrafish model with conditional myc-induced T cell acute lymphoblastic leukemia. *Proc. Natl. Acad. Sci. USA* **102**, 6068-6073.

Lee, J. S. and Thorgeirsson, S. S. (2004). Genome-scale profiling of gene expression in hepatocellular carcinoma: classification, survival prediction, and identification of therapeutic targets. *Gastroenterology* **127 Suppl. 1**, S51-S55.

Lee, J. S., Chu, I. S., Mikaelyan, A., Calvisi, D. F., Heo, J., Reddy, J. K. and Thorgeirsson, S. S. (2004). Application of comparative functional genomics to identify best-fit mouse models to study human cancer. *Nat. Genet.* **36**, 1306-1311.

Li, Z., Huang, X., Zhan, H., Zeng, Z., Li, C., Spitsbergen, J. M., Meierjohann, S., Schartl, M. and Gong, Z. (2012). Inducible and repressable oncogene-addicted hepatocellular carcinoma in Tet-on xmrk transgenic zebrafish. *J. Hepatol.* **56**, 419-425.

Lieschke, G. J. and Currie, P. D. (2007). Animal models of human disease: zebrafish swim into view. *Nat. Rev. Genet.* **8**, 353-367.

Lindström, M. S. (2009). Emerging functions of ribosomal proteins in gene-specific transcription and translation. *Biochem. Biophys. Res. Commun.* **379**, 167-170.

Liu, S. and Leach, S. D. (2011). Zebrafish models for cancer. *Annu. Rev. Pathol.* **6**, 71-93.

Menescal, L. A., Schmidt, C., Liedtke, D. and Schartl, M. (2012). Liver hyperplasia after tamoxifen induction of Myc in a transgenic medaka model. *Dis. Model. Mech.* **5**, 492-502.

Mortazavi, A., Williams, B. A., McCue, K., Schaeffer, L. and Wold, B. (2008). Mapping and quantifying mammalian transcriptomes by RNA-Seq. *Nat. Methods* **5**, 621-628.

Nguyen, A. T., Emelyanov, A., Koh, C. H., Spitsbergen, J. M., Lam, S. H., Mathavan, S., Parinov, S. and Gong, Z. (2011). A high level of liver-specific expression of oncogenic Kras(V12) drives robust liver tumorigenesis in transgenic zebrafish. *Dis. Model. Mech.* **4**, 801-813.

Nguyen, A. T., Emelyanov, A., Koh, C. H., Spitsbergen, J. M., Parinov, S. and Gong, Z. (2012). An inducible kras(V12) transgenic zebrafish model for liver tumorigenesis and chemical drug screening. *Dis. Model. Mech.* **5**, 63-72.

Nordenstedt, H., White, D. L. and El-Serag, H. B. (2010). The changing pattern of epidemiology in hepatocellular carcinoma. *Dig. Liver Dis.* **42 Suppl. 3**, S206-S214.

Payne, E. and Look, T. (2009). Zebrafish modelling of leukaemias. *Br. J. Haematol.* **146**, 247-256.

Rebouissou, S., Imbeaud, S., Balabaud, C., Boulanger, V., Bertrand-Michel, J., Tercé, F., Auffray, C., Bioulac-Sage, P. and Zucman-Rossi, J. (2007). HNF1alpha inactivation promotes lipogenesis in human hepatocellular adenoma independently of SREBP-1 and carbohydrate-response element-binding protein (ChREBP) activation. *J. Biol. Chem.* **282**, 14437-14446.

Rebouissou, S., Amessou, M., Couchy, G., Poussin, K., Imbeaud, S., Pilati, C., Izard, T., Balabaud, C., Bioulac-Sage, P. and Zucman-Rossi, J. (2009). Frequent in-frame somatic deletions activate gp130 in inflammatory hepatocellular tumours. *Nature* **457**, 200-204.

Roessler, S., Jia, H. L., Budhu, A., Forgues, M., Ye, Q. H., Lee, J. S., Thorgeirsson, S. S., Sun, Z., Tang, Z. Y., Qin, L. X. et al. (2010). A unique metastasis gene signature enables prediction of tumor relapse in early-stage hepatocellular carcinoma patients. *Cancer Res.* **70**, 10202-10212.

Ruggero, D. and Pandolfi, P. P. (2003). Does the ribosome translate cancer? *Nat. Rev. Cancer* **3**, 179-192.

Saeed, A. I., Sharov, V., White, J., Li, J., Liang, W., Bhagabati, N., Braisted, J., Klapa, M., Currier, T., Thiagarajan, M. et al. (2003). TM4: a free, open-source system for microarray data management and analysis. *Biotechniques* **34**, 374-378.

Saeed, A. I., Bhagabati, N. K., Braisted, J. C., Liang, W., Sharov, V., Howe, E. A., Li, J., Thiagarajan, M., White, J. A. and Quackenbush, J. (2006). TM4 microarray software suite. *Methods Enzymol.* **411**, 134-193.

Sawey, E. T., Chanrion, M., Cai, C., Wu, G., Zhang, J., Zender, L., Zhao, A., Busuttil, R. W., Yee, H., Stein, L. et al. (2011). Identification of a therapeutic strategy targeting amplified FGF19 in liver cancer by oncogenomic screening. *Cancer Cell* **19**, 347-358.

Shachaf, C. M., Kopelman, A. M., Arvanitis, C., Karlsson, A., Beer, S., Mandl, S., Bachmann, M. H., Borowsky, A. D., Ruebner, B., Cardiff, R. D. et al. (2004). MYC inactivation uncovers pluripotent differentiation and tumour dormancy in hepatocellular cancer. *Nature* **431**, 1112-1117.

Subramanian, A., Tamayo, P., Mootha, V. K., Mukherjee, S., Ebert, B. L., Gillette, M. A., Paulovich, A., Pomeroy, S. L., Golub, T. R., Lander, E. S. et al. (2005). Gene set enrichment analysis: a knowledge-based approach for interpreting genome-wide expression profiles. *Proc. Natl. Acad. Sci. USA* **102**, 15545-15550.

van Riggelen, J., Yetil, A. and Felsher, D. W. (2010). MYC as a regulator of ribosome biogenesis and protein synthesis. *Nat. Rev. Cancer* **10**, 301-309.

van Ruissen, F., Ruijter, J. M., Schaaf, G. J., Asgharnegad, L., Zwijnenburg, D. A., Kool, M. and Baas, F. (2005). Evaluation of the similarity of gene expression data estimated with SAGE and Affymetrix GeneChips. *BMC Genomics* **6**, 91.

Wurmbach, E., Chen, Y. B., Khitrov, G., Zhang, W., Roayaie, S., Schwartz, M., Fiel, I., Thung, S., Mazzaferro, V., Bruix, J. et al. (2007). Genome-wide molecular profiles of HCV-induced dysplasia and hepatocellular carcinoma. *Hepatology* **45**, 938-947.

Zeller, K. I., Jegga, A. G., Aronow, B. J., O'Donnell, K. A. and Dang, C. V. (2003). An integrated database of genes responsive to the Myc oncogenic transcription factor: identification of direct genomic targets. *Genome Biol.* **4**, R69.